Supporting Information for Photocatalytic Deoxygenation of N–O bonds with Rhenium Complexes: from the Reduction of Nitrous Oxide to Pyridine *N*-Oxides

Marianne Kjellberg, Alexia Ohleier, Pierre Thuéry, Emmanuel Nicolas, Lucile Anthore-Dalion,* and Thibault Cantat*

NIMBE, CEA, CNRS, Université Paris-Saclay, CEA Saclay, 91191 Gif sur Yvette Cedex
Tel: +33 1 69 08 43 38 ; Fax: +33 1 69 08 66 40
E-mail: lucile.anthore@cea.fr, thibault.cantat@cea.fr

1 Supplementary Data

1.1 Control experiments for the photocatalytic reduction of pyridine *N*-oxide 1a

*Table S1: Photocatalytic reduction of pyridine N-oxide **1a** and control experiments*

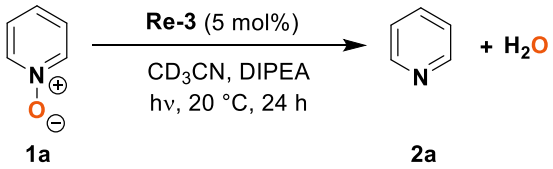

Entry	Deviation from standard conditions[a]	Conversion of 1a (%)[b]	Yield of 2a (%)[b]
1	None	100	78
2	No light	0	0
3	No photocatalyst	0	0
4	No pyridine *N*-oxide	0	0
5	No DIPEA	0	0

[a] Standard reaction conditions: **1a** (100 µmol), **Re-3** (5 µmol, 5 mol%), CD_3CN (0.5 mL), DIPEA (0.1 mL, 570 µmol, 5.7 equiv), 20 °C, 24 h of irradiation.
[b] Conversions and yields measured by ^1H NMR analysis of the crude reaction mixture (internal standard: mesitylene).

1.2 Photocatalytic reduction of 4-cyanopyridine *N*-oxide 1f

In the case of the photocatalytic reduction of **1f**, the conversion to **2f** was maximal (77%) after 30 minutes of irradiation. Further irradiation of the same NMR tube afforded pyridine **2a** in 100% conversion after 8 hours (Figure S1). The decyanation of **2f** to **2a** by irradiation of $[Re(bpy)(CO)_3(\mathbf{2f})]^+$ in DMF:TEOA was reported by the group of Ishitani, affording $[Re(bpy)(CO)_3(CN)]$ and free pyridine **2a**.[1] Thus, the conversion of **2f** to **2a** observed here is proposed to occur *via* the formation of intermediate $[Re(bpy)(CO)_3(\mathbf{2f})]^+$.

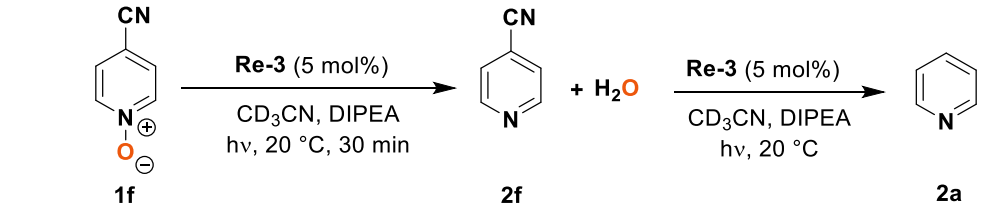

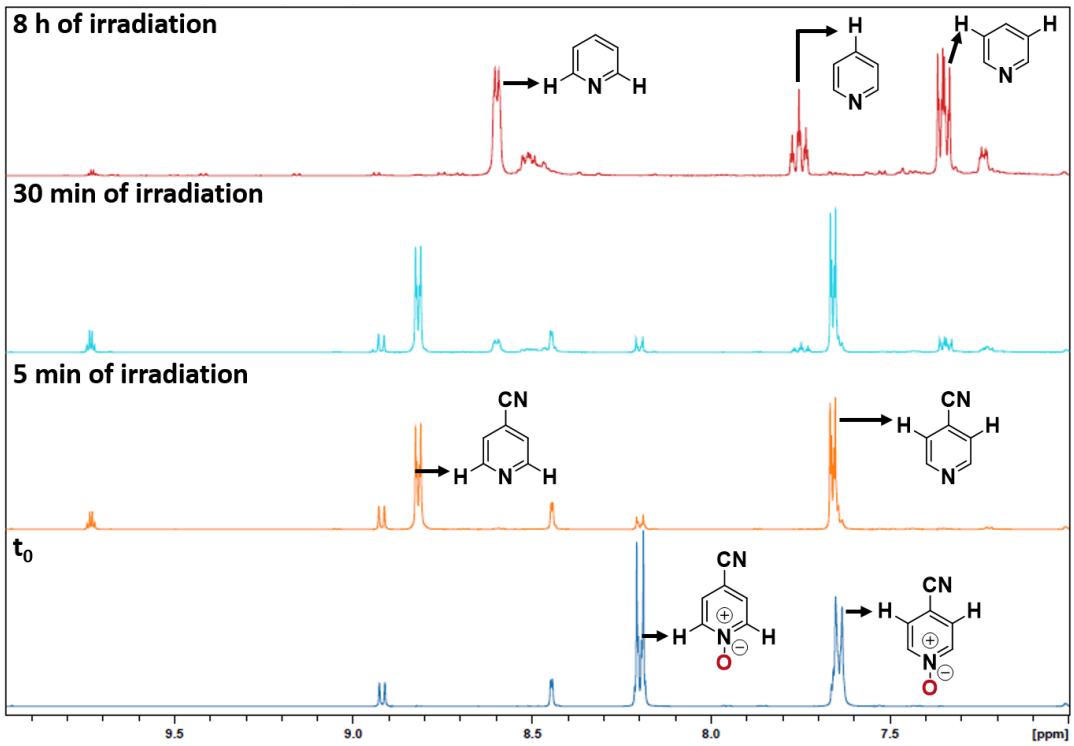

*Figure S1: Photocatalytic reduction of 4-cyanopyridine N-oxide **1f** with **Re-3**: evolution of the reaction mixture (^{1}H NMR, aromatic region).*

1.3 Influence of an external chloride source

A control experiment was realized to study the influence of the addition of a chloride source on the photocatalytic reaction. In a glovebox, an NMR tube equipped with a *J. Young* valve was charged with [Re(bpy)(CO)$_3$Cl] **Re-1** (2.3 mg, 5 µmol, 5 mol%), followed by CD_3CN (0.5 mL), DIPEA (0.1 mL, 570 µmol, 5.7 equiv) and NEt_4Cl.(16.6 mg, 100 µmol, 1 equiv). The reaction mixture was degassed by 3 freeze-pump-thaw cycles and exposed to a N_2O atmosphere (1 bar, ca. 100 µmol, ca. 2.4 mL, 1 equiv.). The tube was left 2 hours under irradiation. The gaseous fraction was analyzed by GC (Figure S2). The reaction afforded 98% yield in N_2.

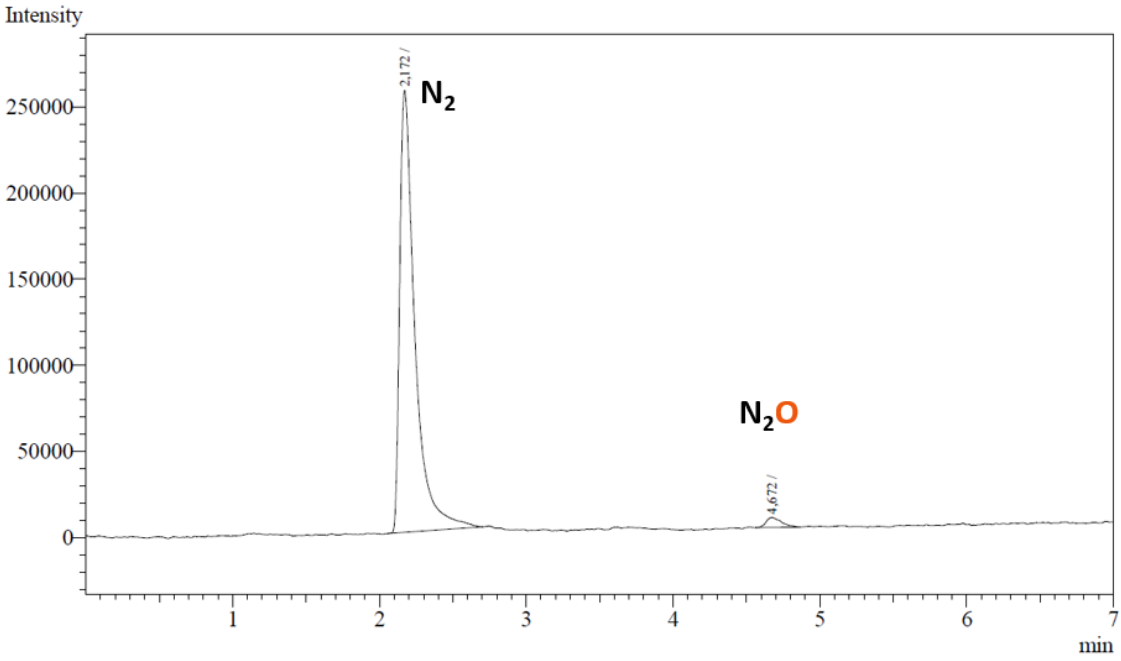

Figure S2: GC trace after 2 h of irradiation of the control experiment with DIPEA and addition of 1 equiv. NEt_4Cl

2 Experimental Details

2.1 Material and methods

2.1.1 General

All reactions and manipulations were performed at 20 °C in a recirculating mBraun LabMaster DP inert atmosphere (Ar) drybox and/or using Schlenk lines. Glassware was dried overnight at 120 °C. Unless otherwise stated, all the reagents were purchased from commercial suppliers (Aldrich, Acros, Alfa Aesar, TCI). Nitrous oxide was purchased from Messer (purity ≥ 99,998%). Non deuterated solvents were thoroughly dried and distilled by standard methods prior to use. Deuterated solvents were dried on molecular sieves (4 Å; Aldrich) before use. ^{1}H and ^{13}C NMR spectra were recorded on a Bruker Advance Neo spectrometer operating at 400 MHz for ^{1}H. Chemical shifts for ^{1}H and $^{13}C\{^{1}H\}$ NMR spectra were referenced to solvent impurities. Coupling constants *J* are given in Hz. The following abbreviations are used: s, singlet; d, doublet; t, triplet; m, multiplet. Gas chromatography data were collected on a Shimadzu GC-2010 Plus. UV-visible spectra were recorded on a PerkinElmer Lambda 900 spectrometer.

2.1.2 Experimental setup for irradiation

A custom-made irradiation setup was used for all photocatalytic experiments. It is constituted of a hexagonal aluminum chassis with 6 regularly disposed holes, one on each side. A Light Emitting Diode (cool white LED, GU5.3 / MR16 12V 8W SMD 80°, 6000-8000 K) is built into each hole. On top, the apparatus displays 6 equivalent positions that can host NMR tubes for reproducible irradiations, and one hole in the middle used for scale-up experiments (Figure S3, right). A cooling fan under the reactor enables to evacuate the heat produced by the absorbing solution and/or by exothermic reactions. The whole apparatus is supported by a magnetic stirrer; stirring enables to maximize the absorption of photons by the solution. In our experiments, stirring was performed at 300 rpm.

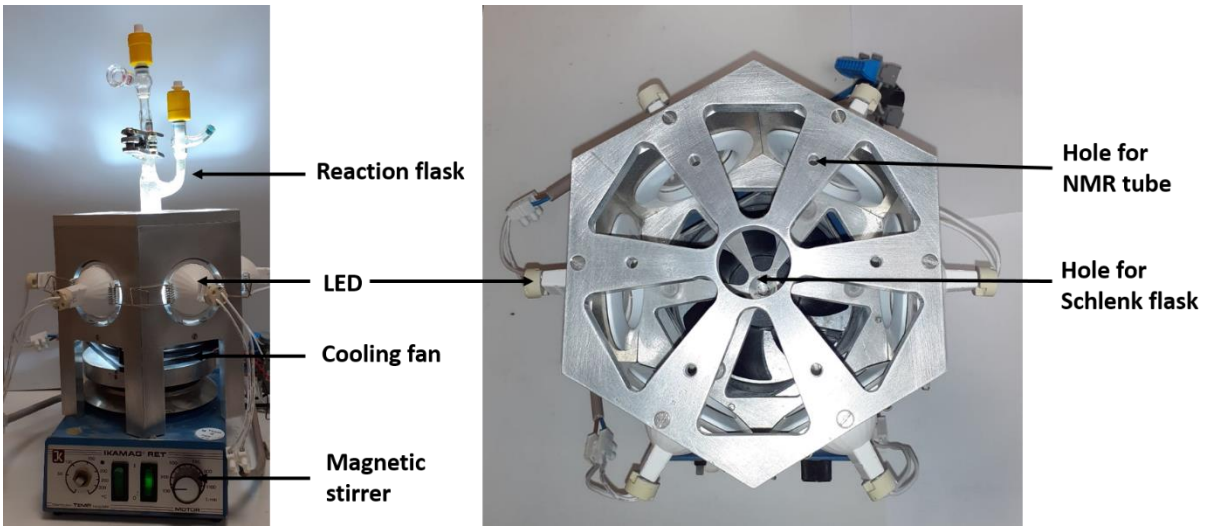

Figure S3: Sideview (left) and topview (right) of the setup used for irradiation.

2.2 Synthetic procedures for catalysts

Complexes **Re-1** to **Re-3** were prepared according to reported procedures.[2] The NMR data are in agreement with those reported in the literature.[3] Complexes **Re-4** and **Re-5** were synthesized using the same methodology.

2.2.1 Synthesis of [Re(6,6'-dmb)(CO)$_3$Cl] **Re-4**

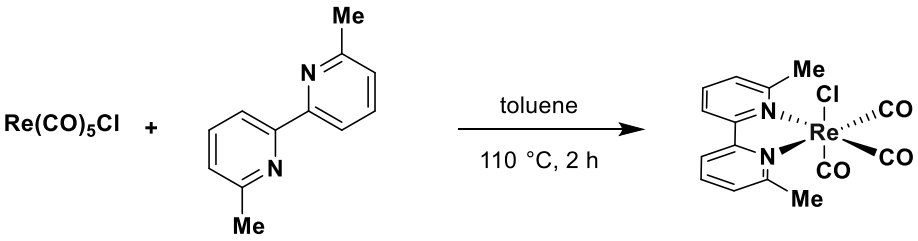

Scheme S1: Synthetic pathway towards [Re(6,6'-dmb)(CO)$_3$Cl] ***Re-4****.*

In a glovebox, a 50 mL round-bottomed flask equipped with a stirring bar and a *J-Young* valve was charged with 6,6'-dimethylbipyridine (88 mg, 478 µmol, 1 equiv.), [Re(CO)$_5$Cl] (173 mg, 478 µmol, 1 equiv.), and 15 mL of anhydrous toluene. The flask was sealed, brought out of the glovebox, and immersed in an oil bath at 110 °C. After 2 hours, the resulting yellow solution was cooled down to room temperature and the solvent was removed *in vacuo* to afford a crude yellow solid. The latter was suspended in pentane and centrifuged three times for 10 min. The solid was dried under vacuum overnight to give [Re(6,6'-dimethylbipyridine)(CO)$_3$Cl] **Re-4** (170 mg, 73%) as a yellow powder. Single crystals suitable for X-ray diffraction were obtained by slow diffusion of pentane into a THF solution of **Re-4** at room temperature.

The NMR, IR and UV-visible data for **Re-4** are in agreement with that reported in the literature.[4]

^{1}H NMR (400 MHz, CD_2Cl_2) δ 8.01 (d, J = 8.0 Hz, 2H), 7.92 (t, J = 7.9 Hz, 2H), 7.47 (d, J = 7.4 Hz, 2H), 3.10 (s, 6H), ppm

^{13}C NMR (400 MHz, CD_2Cl_2) δ 163.0, 158.3, 139.4, 126.9, 121.3, 30.4 ppm

IR ν(CO): 2013, 1894, 1881 cm^{-1}

UV-Vis (acetonitrile) λ_{max} (ε) = 315 (6270), 329 (5330), 355 nm (1760 $M^{-1}.cm^{-1}$)

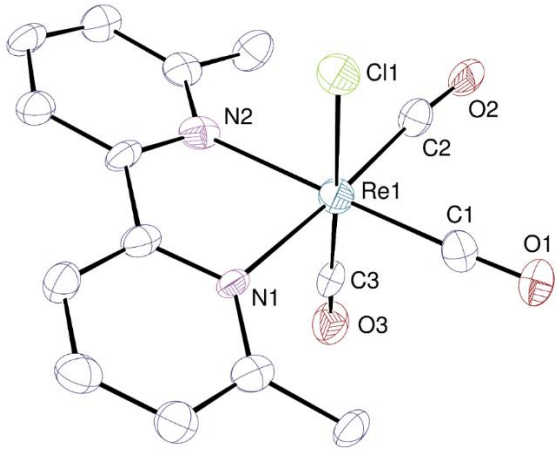

*Figure S4: View of **Re-4** with displacement ellipsoids drawn at the 50% probability level and hydrogen atoms omitted.*

2.2.2 Synthesis of [Re(6,6'-mesbpy)$(CO)_3$Cl] **Re-5**

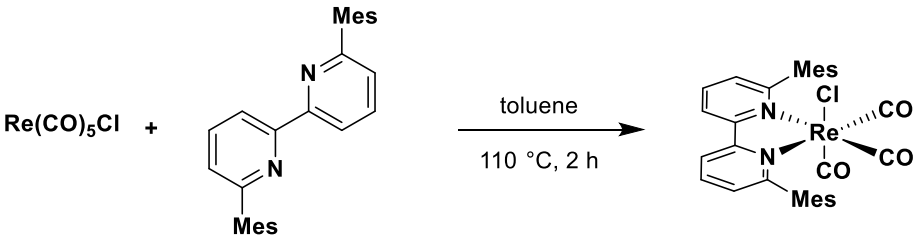

*Scheme S2: Synthetic pathway towards [Re(6,6'-mesbpy)$(CO)_3$Cl] **Re-5.***

Synthesis of 6,6'-dimesityl-2,2'-bipyridine (mesbpy) was performed as previously reported by the Suzuki coupling of 6,6'-dibromo-2,2'-bipyridine with mesitylboronic acid.[5]

[Re(6,6'-mesbpy)$(CO)_3$Cl] **Re-5** was prepared as follows: in a glovebox, a 50 mL round-bottomed flask equipped with a stirring bar and a *J. Young* valve was charged with 6,6'-dimesityl-2,2'-bipyridine (140 mg, 357 mmol, 1 equiv.), [$Re(CO)_5Cl$] (130 mg, 359 mmol, 1 equiv.), and 15 mL of anhydrous toluene. The flask was sealed, brought out of the glovebox, and immersed in an oil bath at 110 °C. After 2 hours, the resulting yellow solution was cooled down to room temperature, and the solvent was removed *in vacuo*. The resulting crude yellow solid was purified by column chromatography on silica

gel (DCM:MeOH 99:1). The solid obtained after evaporation of the solvent was suspended in pentane and centrifuged three times for 10 min. The solid was dried under vacuum overnight to give [Re(6,6'-dimesitylbipyridine)$(CO)_3Cl$] **Re-5** (170 mg, 68%) as a yellow powder. Single crystals suitable for X-ray diffraction were obtained by slow diffusion of pentane into a THF solution of **Re-5** at room temperature.

^{1}H NMR (400 MHz, CD_2Cl_2) δ 8.29 (d, J = 8.3 Hz, 2H), 8.10 (t, J = 7.9 Hz, 2H), 7.40 (d, J = 7.7 Hz, 2H), 6.98 (s, 4H), 2.34 (s, 6H), 2.15 (s, 6H), 2.00 (s, 6H) ppm

^{13}C NMR (400 MHz, CD_2Cl_2) δ 192.3, 190.1, 164.3, 158.0, 139.6, 139.0, 138.7, 136.4, 135.4, 128.9, 128.3, 122.4, 20.9, 20.8, 20.1 ppm

IR ν(CO): 2016, 1918, 1897 cm^{-1}

UV-Vis (acetonitrile) λ_{max} (ε) = 315 (7150), 329 (5940), 370 nm (1400 $M^{-1}.cm^{-1}$)

Elemental analysis calcd (%) for $C_{31}H_{28}ClN_2O_3Re$ (698.13): C 53.33, H 4.04, N 4.01; found: C 53.60, H 3.88, N 3.97.

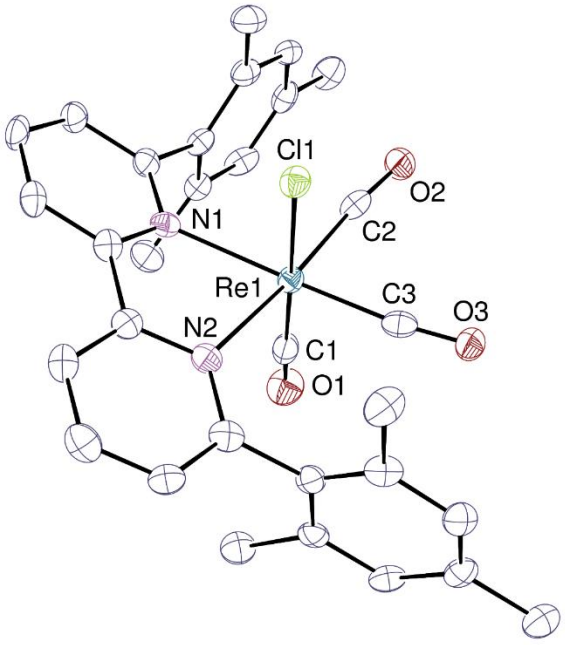

*Figure S5: View of **Re-5** with displacement ellipsoids drawn at the 50% probability level and hydrogen atoms omitted.*

2.3 Photocatalytic procedures

2.3.1 Photocatalytic reduction of N_2O on NMR scale

The procedure is detailed with photocatalyst [Re(bpy)$(CO)_3$Cl] **Re-1**. In a glovebox, a 3 mL NMR tube equipped with a *J. Young* valve was charged with [Re(bpy)$(CO)_3$Cl] **Re-1** (2.3 mg, 5 µmol, 5 mol%), followed by CD_3CN (0.5 mL) and DIPEA (0.1 mL, 570 µmol, 5.7 equiv). The tube was sealed and brought out of the glovebox. The reaction mixture was degassed by 3 freeze-pump-thaw cycles and exposed to a N_2O atmosphere (1 bar, ca. 100 µmol, ca. 2.4 mL, 1 equiv.). The tube was then left 2 hours under irradiation using the setup described in Figure S3. The gaseous fraction was sampled using the setup described in Figure S11 and analyzed by GC to determine the N_2 yield.

2.3.2 Photocatalytic reduction of N_2O on a 1.2 mmol scale

The procedure is detailed with photocatalyst [Re(bpy)$(CO)_3$Cl] **Re-1**. In a glovebox, a Schlenk flask (Figure S6) equipped with two *J. Young* valves, a GC septum (*Supelco*, thermogreen TM LB-2) and a stirring bar was charged with [Re(bpy)$(CO)_3$Cl] **Re-1** (22.4 mg, 60 µmol, 5 mol%), followed by acetonitrile (6 mL) and DIPEA (1.2 mL, 6.9 mmol, 5.7 equiv). The two valves were sealed, and the flask was brought out of the glovebox. The resulting yellow solution was degassed by three freeze-pump-thaw cycles, then exposed to a N_2O atmosphere (1.0 bar, ca. 1.2 mmol, ca. 28.8 mL, 1 equiv.). The flask was left to irradiate in the center of the setup described in Figure S3. At regular intervals valve (*) was opened and 150 µL of the headspace were sampled and analyzed by GC; then, valve (*) was closed.

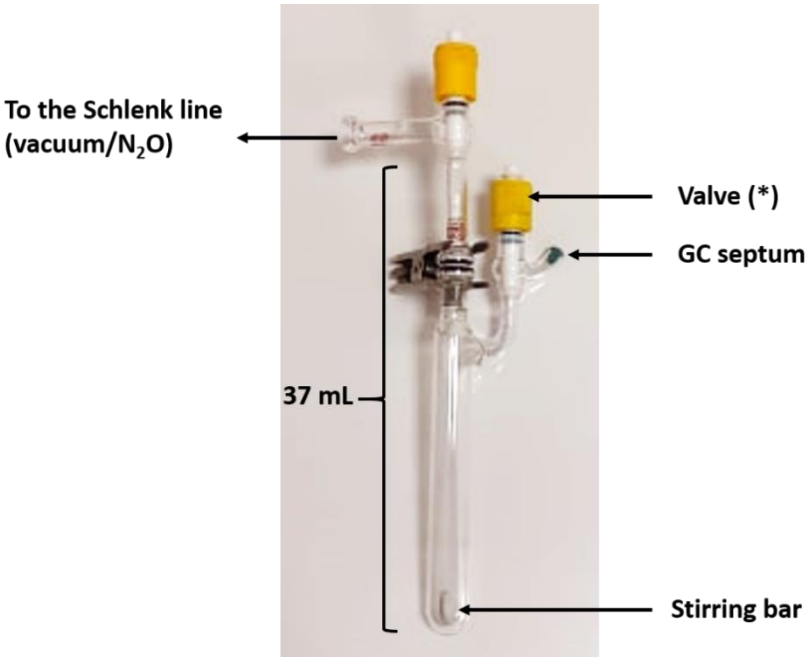

Figure S6: Sideview of the scale-up reaction setup.

TONs for N_2 were calculated as follows:

$$\mathrm{TON} = \frac{\mathrm{n(N_2)}}{\mathrm{n(catalyst)}}$$

where $n(N_2)$ is the final quantity of N_2 in the reaction setup.

The different values of $n(N_2)$ for each catalyst and corresponding TONs are given in Table S2.

Table S2: Calculation of TON N_2 for each catalyst on 1.2 mmol scale. Reaction conditions: N_2O (1.0 bar, 1.2 mmol), photocatalyst (60 µmol, 5 mol%), CH_3CN (6 mL), DIPEA (1.2 mL, 6.9 mmol, 5.7 equiv).

Entry	Catalyst	TOF_0 (h^{-1})	Time of irradiation (h)	$n(N_2)$ (mmol)	% N_2 (TON)
1	**Re-1**	0.7	22	0.3	22 (5)
2	**Re-2**	3.7	50	0.84	70 (14)
3	**Re-3**	4.3	115	1.02	86 (17)
4	**Re-4**	2.7	100	0.66	55 (11)
5	**Re-5**	1.1	150	0.73	61 (12)

2.3.3 Photocatalytic reduction of pyridine *N*-oxides

The procedure is detailed in the case of photocatalyst [Re(tbbpy)$(CO)_3$Cl] **Re-3**:

In a glovebox, a 3 mL NMR tube equipped with a *J. Young* valve was charged with **Re-3** (2.9 mg, 5 mol%), followed by pyridine *N*-oxide (9.5 mg, 100 µmol, 1 equiv.), CD_3CN (0.5 mL), DIPEA (0.1 mL, 570 µmol, 5.7 equiv), and mesitylene as an internal standard (10 µL). The tube was sealed, brought out of the glovebox, then left under irradiation using the setup described in Figure S3. The conversion rate and pyridine yield were determined by ^{1}H NMR integration (protons *ortho* to the nitrogen atom) vs. mesitylene as an internal standard.

Representative NMR spectra for the photocatalytic deoxygenation of pyridine *N*-oxide **1a** with **Re-3** are given in Figure S7. The NMR data for all substituted pyridines are in agreement with those reported in the literature.[6]

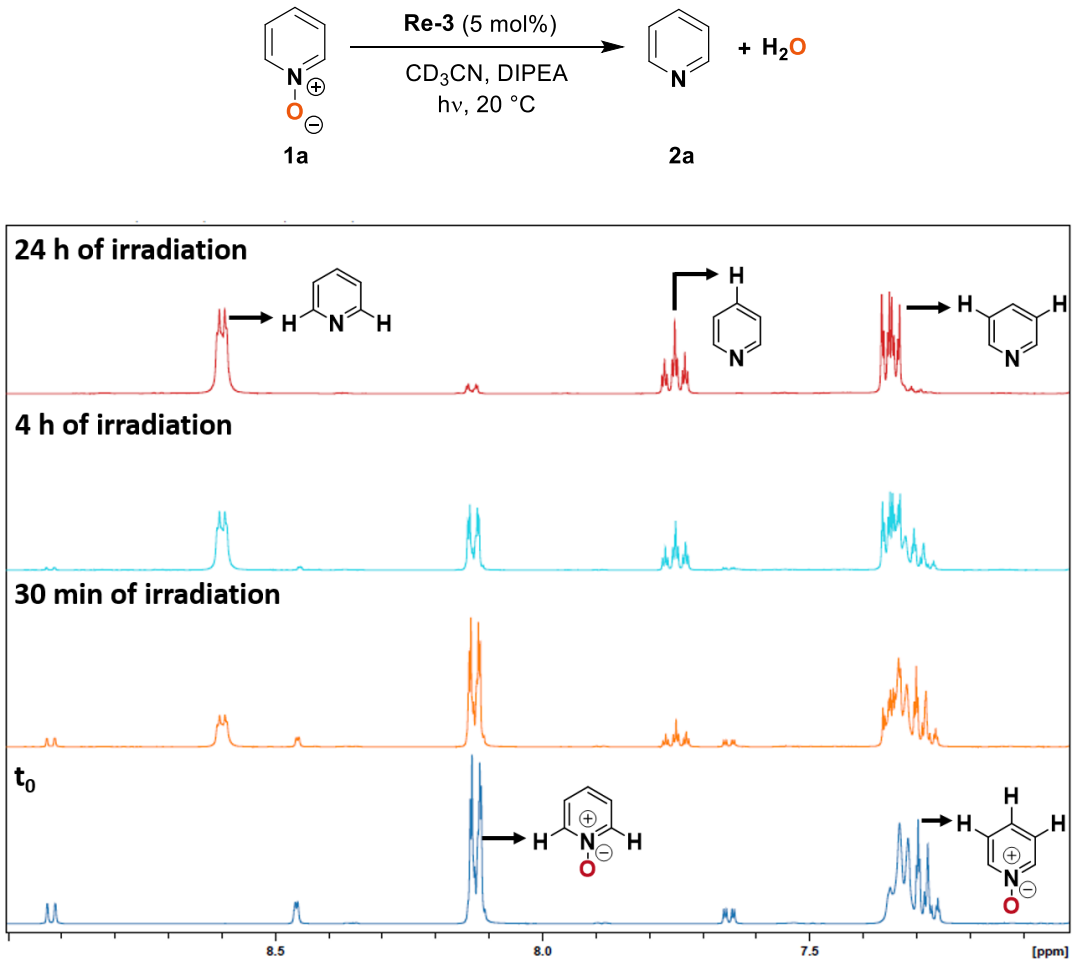

*Figure S7: Photocatalytic reduction of pyridine N-oxide **1a** with **Re-3**: evolution of the reaction mixture (^{1}H NMR, aromatic region).*

2.3.3.1 *Synthesis of 6-methyl-2-(4-octen-4-yl)pyridine from 2-methylpyridine N-oxide **4***

2-methylpyridine was oxidized to 2-methylpyridine *N*-oxide according to a reported literature procedure, then was engaged in a nickel-catalyzed hydroheteroarylation with 4-octyne following the procedure reported by Hiyama *et al.*.[7] The product obtained, 6-methyl-2-(4-octen-yl)pyridine *N*-oxide **5** (E/Z: 93/7), was deoxygenated using the following procedure: in a glovebox, a 3 mL NMR tube equipped with a *J. Young* valve was charged with **Re-3** (2.9 mg, 5 µmol, 5 mol%), followed by, 6-methyl-2-(4-octen-yl)pyridine *N*-oxide (21.9 mg, 100 µmol, 1 equiv.), CD_3CN (0.5 mL), DIPEA (0.1 mL, 570 µmol, 5.7 equiv), and mesitylene as an internal standard (10 µL). The tube was sealed, brought out of the glovebox, then left under irradiation using the setup described in Figure S3. The conversion rate and pyridine yield were determined by ^{1}H NMR integration (alkene proton) vs. mesitylene as an internal standard. The reaction afforded 6-methyl-2-(4-octen-4-yl)pyridine **3** in 82% yield after 8 h of irradiation. The NMR data are in agreement with those reported in the literature.[7]

3 GC analyses

3.1 GC conditions

Column: Carboxen 1010 Plot fused silica capillary column (30 m × 0.53 mm × 30 µm); injection temperature: 230 °C; column temperature: 150 °C; flow: 5 mL/min; purge: 2 mL/min; split ratio: 5.0; carrier gas: argon; detector: TCD 230 °C, 30 mA.

3.2 GC calibration

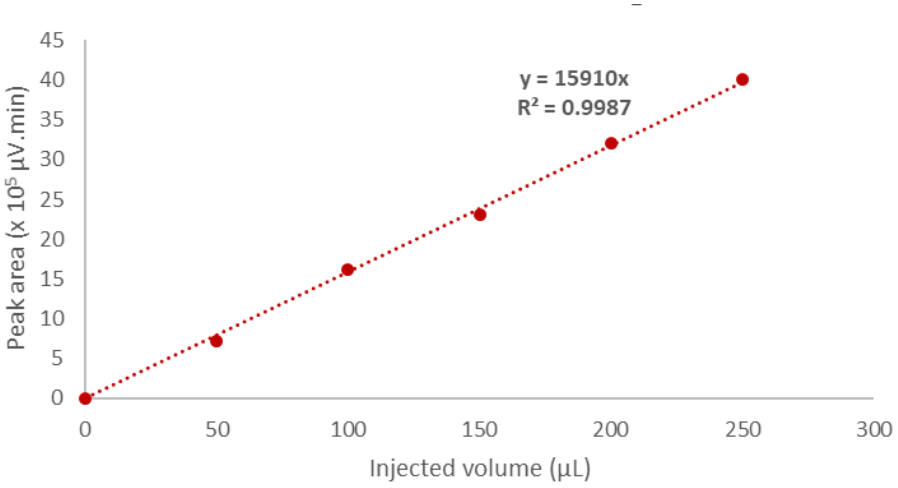

Figure S8: GC Calibration curve for N_2.

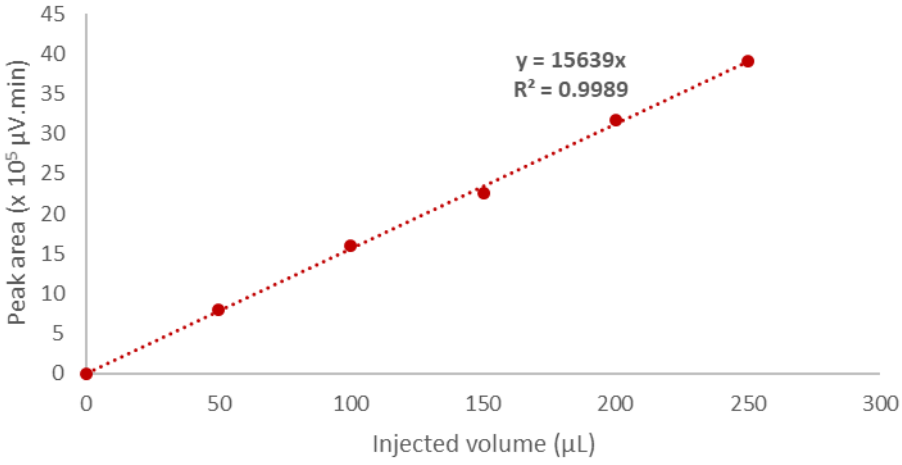

Figure S9: GC Calibration curve for N_2O.

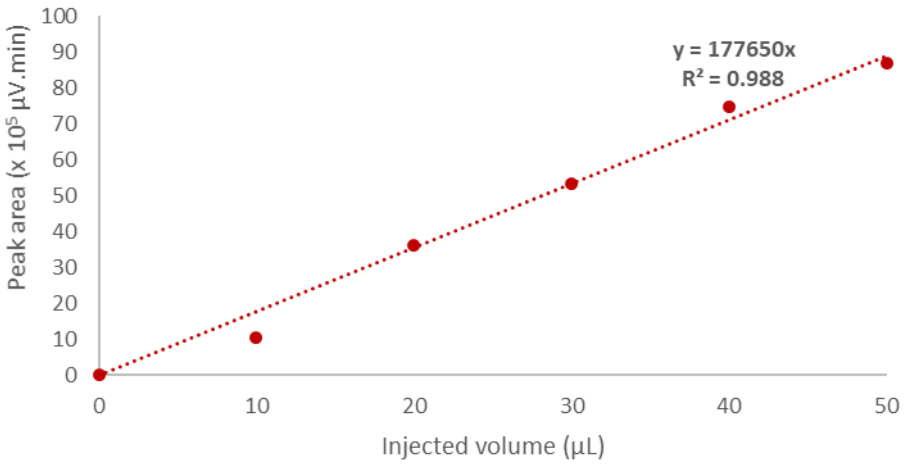

Figure S10: GC Calibration curve for H_2.

Table S3: Retention times and response coefficients of analyzed species.

Species	Retention time (min)	Response factor (µV.min.µL^{-1})
H_2	1.96	177650
N_2	2.08	15910
N_2O	4.45	15639

3.3 Analysis of the gaseous fraction from a J-Young NMR tube

The *J. Young* NMR tube was connected to a small glass chamber, itself connected to the Schlenk line. The chamber was sealed with a GC septum (*Supelco*, thermogreenTM LB-2, Figure S11) and placed under high vacuum (V = 1 mL, P = 10^{-2} mbar) to limit air contamination. The chamber was closed, and the *J. Young* NMR tube was open, allowing the gaseous phase to expand. The gas phase was sampled through the septum using a *Hamilton® SampleLock* syringe and injected right away into the GC apparatus.

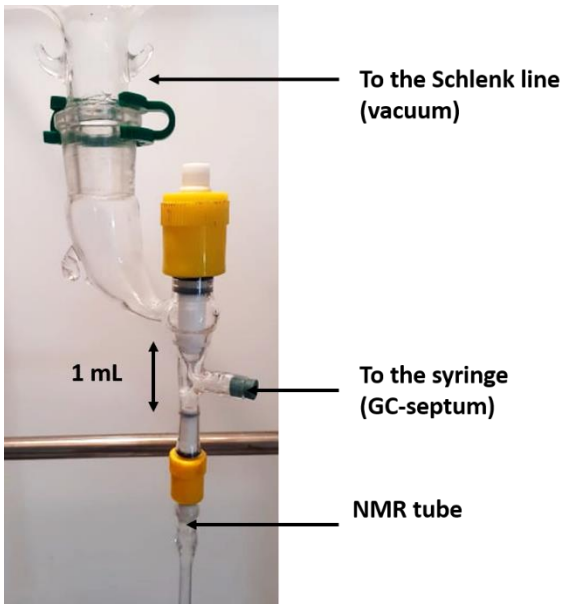

Figure S11: Side view of the apparatus used to analyze the gas phase from a J. Young *NMR tube.*

Table S4: Results of the control experiments.

Entry	Deviation from standard conditions[a]	H_2 (%) [b]	N_2 (%)[b,c]	N_2O (%)[b]
1	None	1.5	66	32
2	No light	0	4	96
3	No photocatalyst	0	2	98
4	Argon instead of N_2O	91	9	0
5	No TEOA	0	8	92
6	DIPEA instead of TEOA	0	76	24

[a] Standard reaction conditions: N_2O (1 bar, 100 µmol), **Re-3** (5 µmol, 5 mol%), CD_3CN (0.5 mL), TEOA (570 µmol, 5.7 equiv), 20 °C, 12 h of irradiation. [b] Determined by GC analysis of the gaseous phase. [c] It was impossible to obtain N_2 levels lower than 2 µL in the blank experiments; that residual amount was attributed to contamination by ambient air between sampling and injection for analysis.

4 Analysis data

4.1 Luminescence quenching experiments

For luminescence quenching experiments, a 1 mM solution of the photocatalyst in dry acetonitrile was prepared in a glovebox filled with argon. Out of the glovebox, the photocatalyst was irradiated: at 370 nm for **Re-1**, at 410 nm for **Re-3**. The change of the luminescence upon addition of DIPEA at different concentrations was recorded. These demonstrated that the luminescence was efficiently quenched by DIPEA for both complexes.

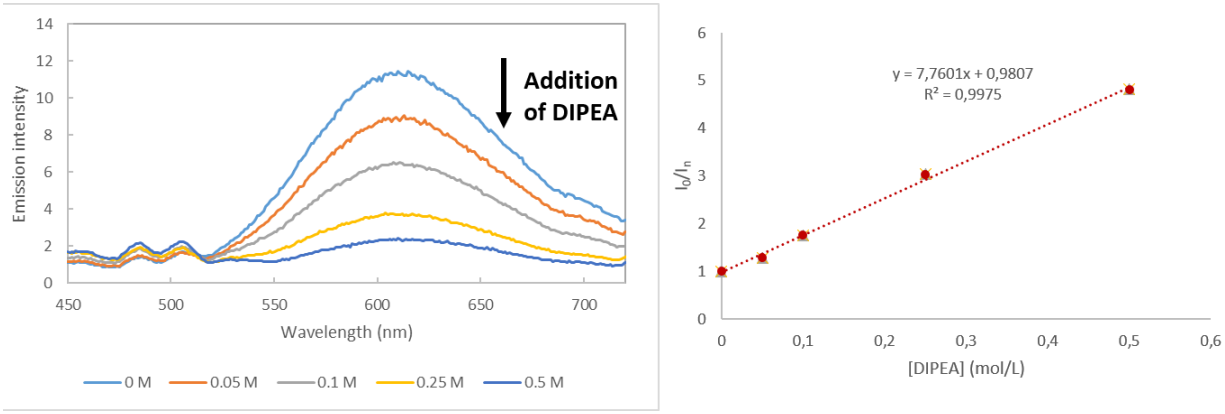

*Figure S12: Changes in the luminescence spectra of **Re-1** upon addition of DIPEA at different concentrations in acetonitrile (left) Stern-Volmer quenching of **Re-1** luminescence with DIPEA (right).*

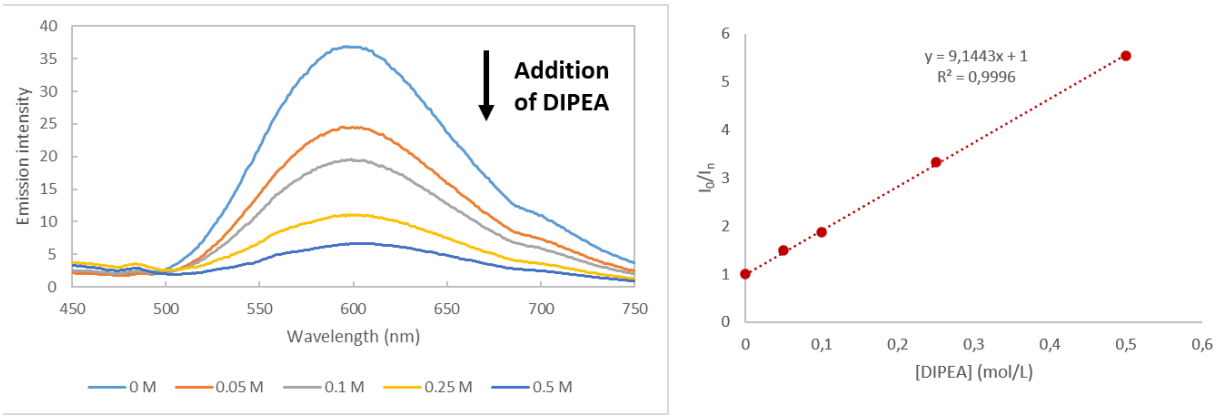

*Figure S13: Changes in the luminescence spectra of **Re-3** upon addition of DIPEA at different concentrations in acetonitrile (left). Stern-Volmer quenching of **Re-3** luminescence with DIPEA (right).*

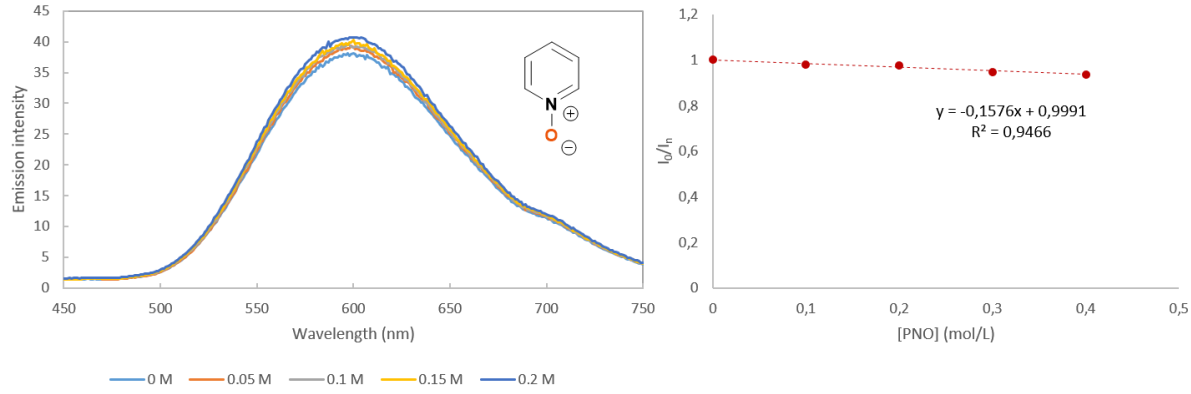

*Figure S14: Changes in the luminescence spectra of **Re-3** upon addition of pyridine N-oxide **1a** at different concentrations in acetonitrile (left). Stern-Volmer quenching of **Re-3** luminescence with pyridine N-oxide **1a** (right)*

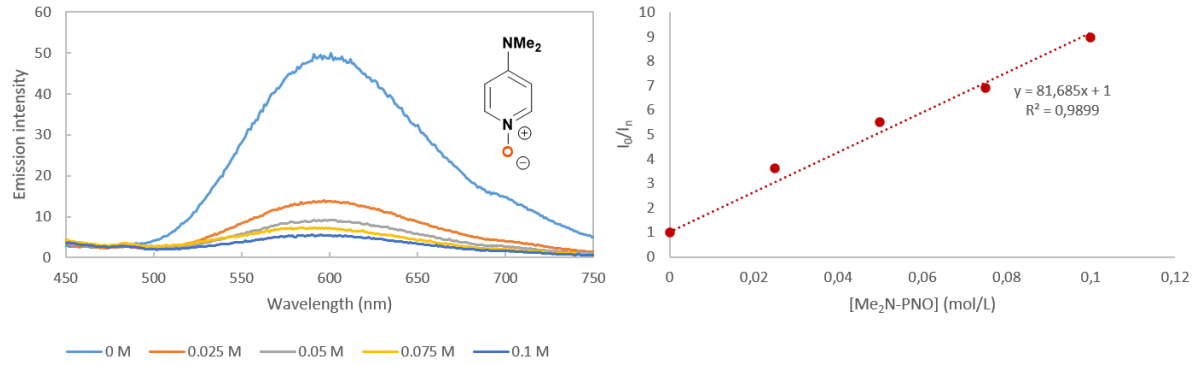

*Figure S15: Changes in the luminescence spectra of **Re-3** upon addition of 4-dimethylaminopyridine N-oxide **1b** at different concentrations in acetonitrile(left). Stern-Volmer quenching of **Re-3** luminescence with 4-dimethylaminopyridine N-oxide **1b** (right)*

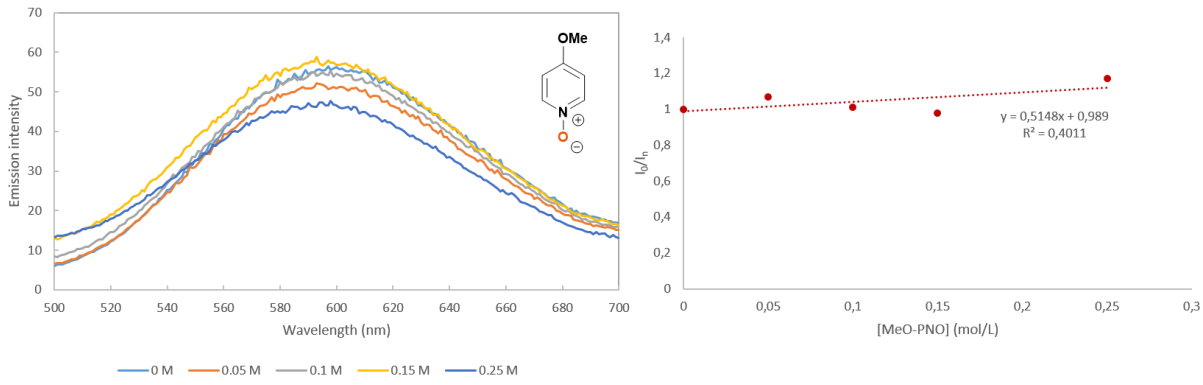

*Figure S16: Changes in the luminescence spectra of **Re-3** upon addition of 4-methoxypyridine* N-*oxide **1c** at different concentrations in acetonitrile(left). Stern-Volmer quenching of **Re-3** luminescence with 4-methoxypyridine* N-*oxide **1c** (right)*

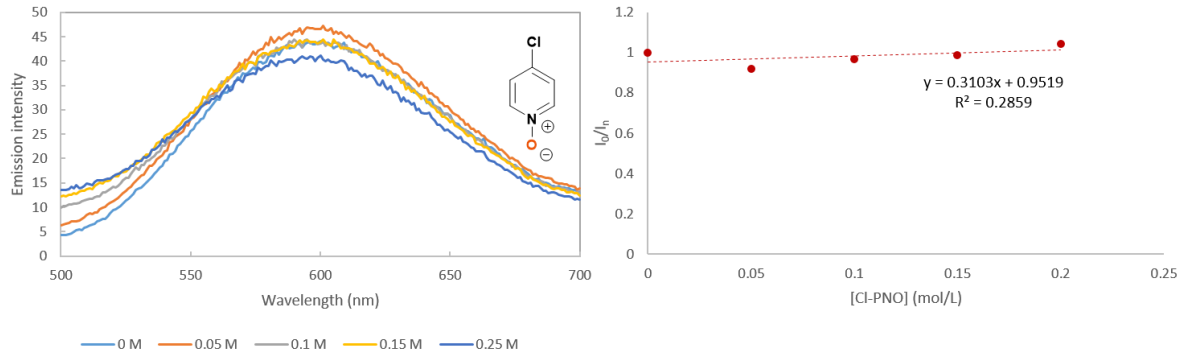

*Figure S17: Changes in the luminescence spectra of **Re-3** upon addition of 4-chloropyridine* N*-oxide **1e** at different concentrations in acetonitrile (left). Stern-Volmer quenching of **Re-3** luminescence with 4-chloropyridine* N*-oxide **1e** (right)*

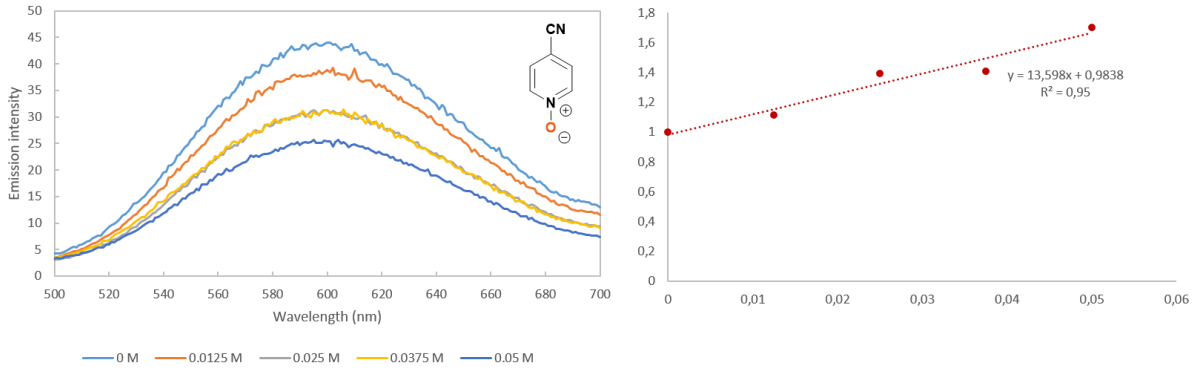

*Figure S18: Changes in the luminescence spectra of **Re-3** upon addition of 4-cyanopyridine* N*-oxide **1f** at different concentrations in acetonitrile (left) Stern-Volmer quenching of **Re-3** luminescence with 4-cyanopyridine* N*-oxide **1f** (right)*

4.2 Crystallography

The data for compound **Re-4**·0.5THF were collected on a *Bruker D8 Quest* diffractometer equipped with an Incoatec Microfocus Source (IμS 3.0 Mo) and a PHOTON III area detector, and operated through the APEX3 software,[8] while those for compound **Re-5**·0.5THF were collected on a Nonius Kappa-CCD area detector diffractometer using graphite-monochromated Mo Kα radiation (λ = 0.71073 Å).[9] The crystals were mounted either into a glass capillary or on a Mitegen micromount with a protective coating of Paratone-N oil (Hampton Research). The data were processed with SAINT (**Re-4**) or HKL2000 (**Re-5**).[10] Absorption effects were corrected empirically with the programs SADABS (**Re-4**) or SCALEPACK (**Re-5**).[10b, 11] All structures were solved by intrinsic phasing with SHELXT,[12] expanded by subsequent difference Fourier synthesis and refined by full-matrix least-squares on F^2 with SHELXL-2014,[13] using the ShelXle interface.[14] All non-hydrogen atoms were refined with anisotropic displacement parameters. The hydrogen atoms were introduced at calculated positions and they were treated as riding atoms with an isotropic displacement parameter equal to 1.2 times that of the parent atom (1.5 for CH_3, with optimized geometry). The solvent THF molecule has twofold rotation symmetry

in **Re-4**·0.5THF while that in **Re-5**·0.5THF is disordered around an inversion center and has been given an occupancy parameter of 0.5 accordingly. The molecular plots were drawn with ORTEP-3.[15]

Crystal data for compound Re-4·0.5THF. $C_{17}H_{16}ClN_2O_{3.5}Re$, M = 525.97, orthorhombic, space group *Pbcn*, a = 13.4935(10), b = 22.1756(17), c = 11.2515(8) Å, V = 3366.8(4) Å^3, Z = 8, D_c = 2.075 g cm^{-3}, μ = 7.399 mm^{-1}, F(000) = 2016. Refinement of 224 parameters on 3201 independent reflections out of 41305 measured reflections (R_{int} = 0.051) led to R_1 = 0.052, wR_2 = 0.114, S = 1.506, $\Delta\rho_{min}$ = –2.09, $\Delta\rho_{max}$ = 1.91 e Å^{-3}.

Crystal data for compound Re-5·0.5THF. $C_{33}H_{32}ClN_2O_{3.5}Re$, M = 734.25, monoclinic, space group *C*2/*c*, a = 35.2615(16), b = 8.1575(3), c = 22.7433(10) Å, β = 116.166(3)°, V = 5871.6(5) Å^3, Z = 8, D_c = 1.661 g cm^{-3}, μ = 4.269 mm^{-1}, F(000) = 2912. Refinement of 394 parameters on 5550 independent reflections out of 155149 measured reflections (R_{int} = 0.065) led to R_1 = 0.030, wR_2 = 0.061, S = 1.101, $\Delta\rho_{min}$ = –1.01, $\Delta\rho_{max}$ = 1.66 e.Å^{-3}.

4.3 Copies of NMR spectra

4.3.1 **Re-4**

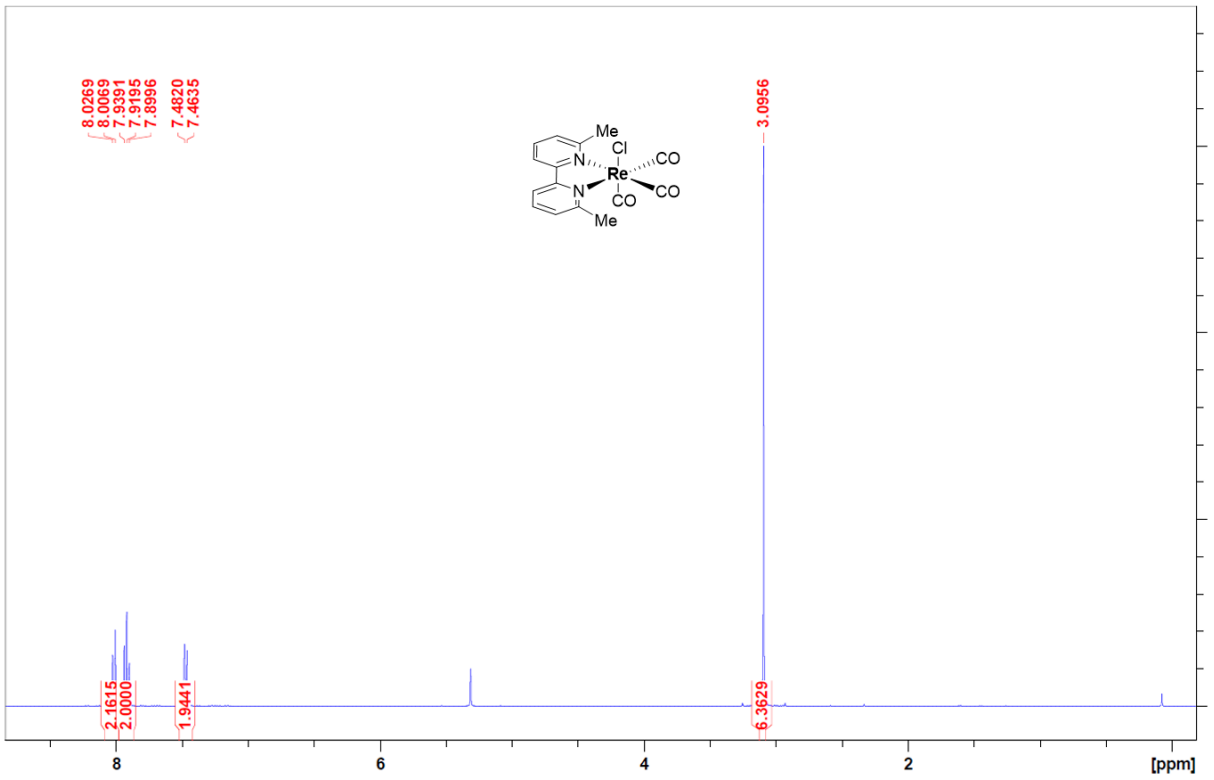

*Figure S19: ^{1}H NMR spectrum of **Re-4** in CD_2Cl_2.*

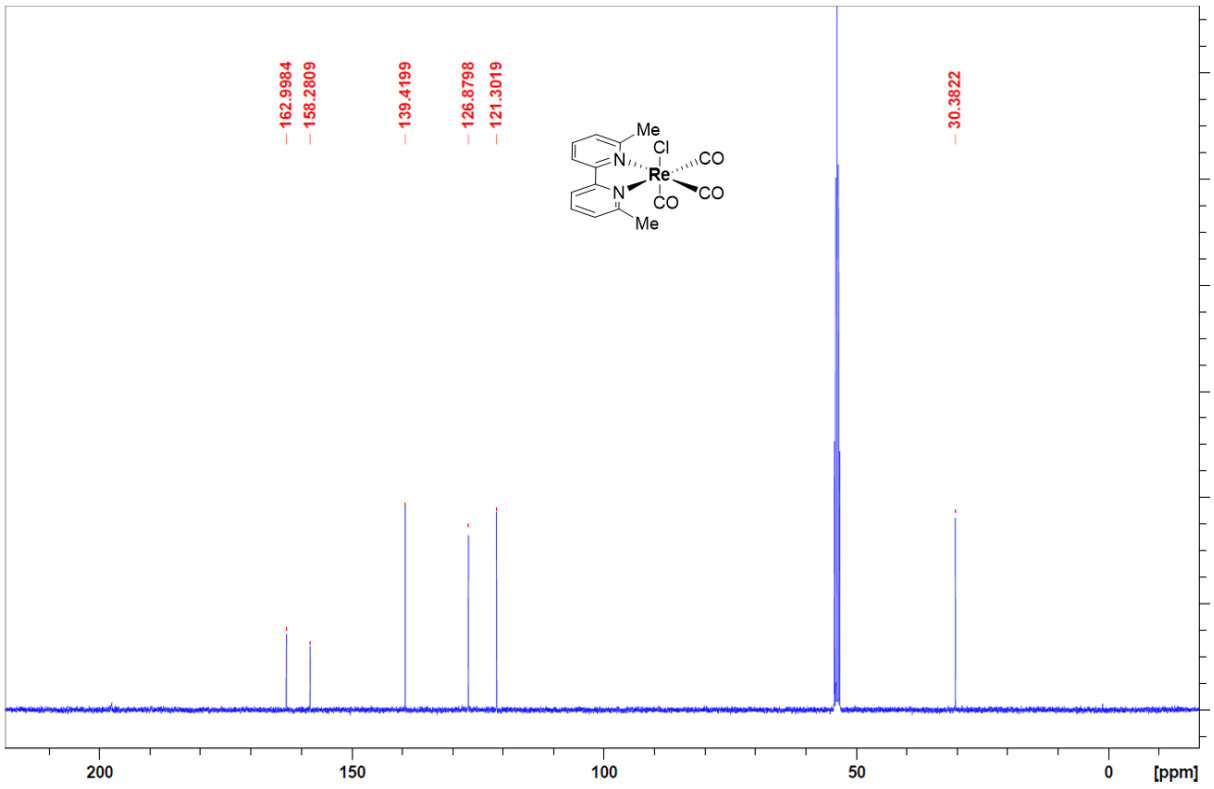

*Figure S20: ^{13}C NMR spectrum of **Re-4** in CD_2Cl_2.*

4.3.2 **Re-5**

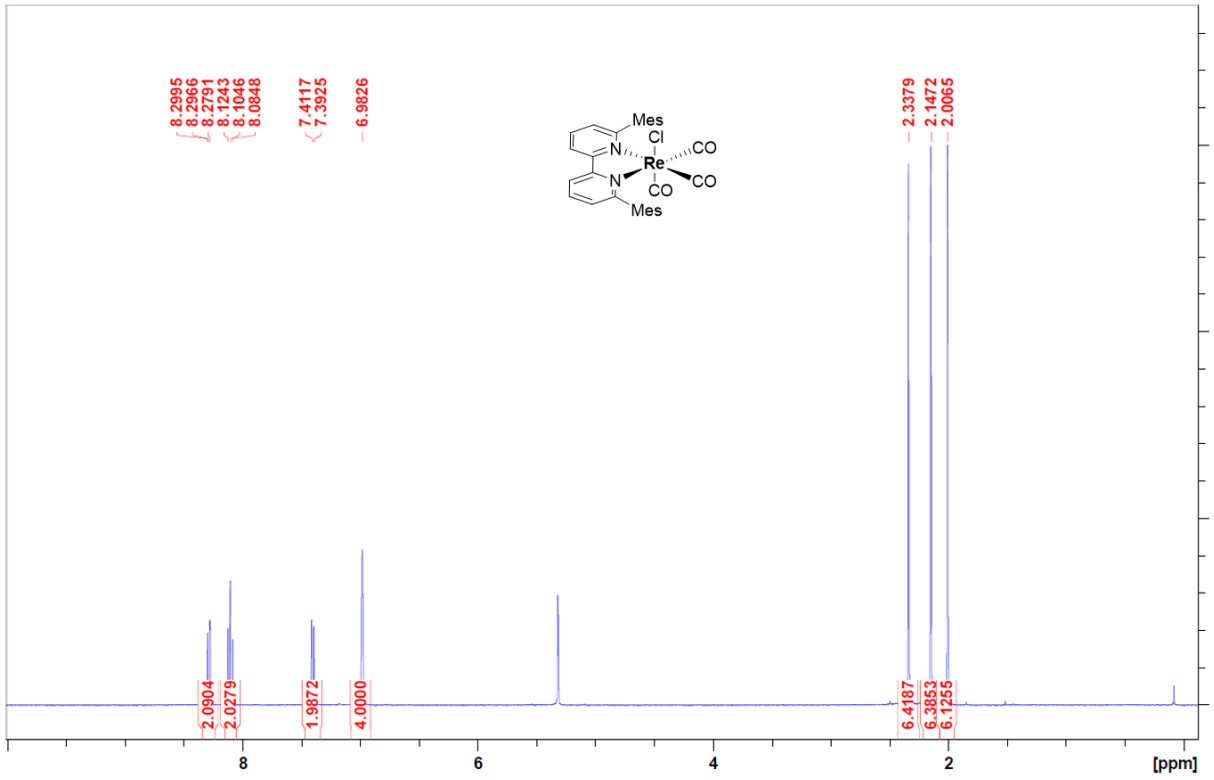

*Figure S21: ^{1}H NMR spectrum of **Re-5** in CD_2Cl_2.*

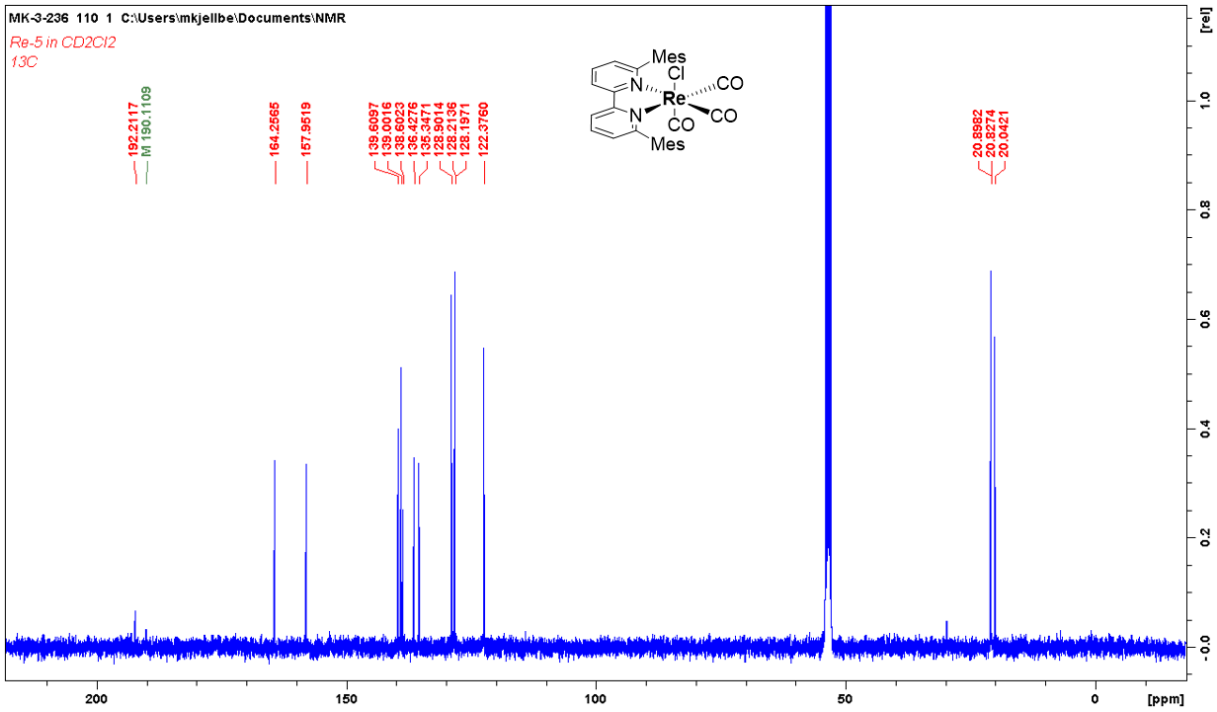

*Figure S22: ^{13}C NMR spectrum of **Re-5** in CD_2Cl_2.*

4.4 Copies of GC traces

4.4.1 Representative GC traces for the photocatalyzed reduction of N_2O by **Re-3**

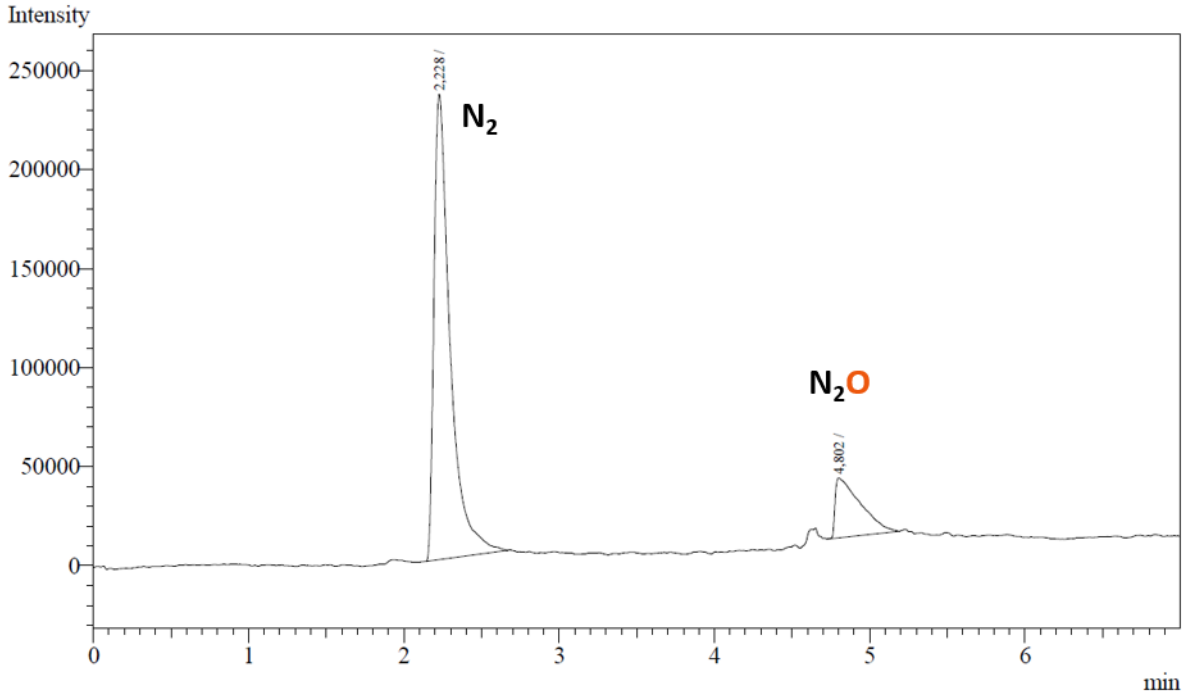

Figure S23: GC analysis of the gaseous phase after 24 h of irradiation, on NMR scale.

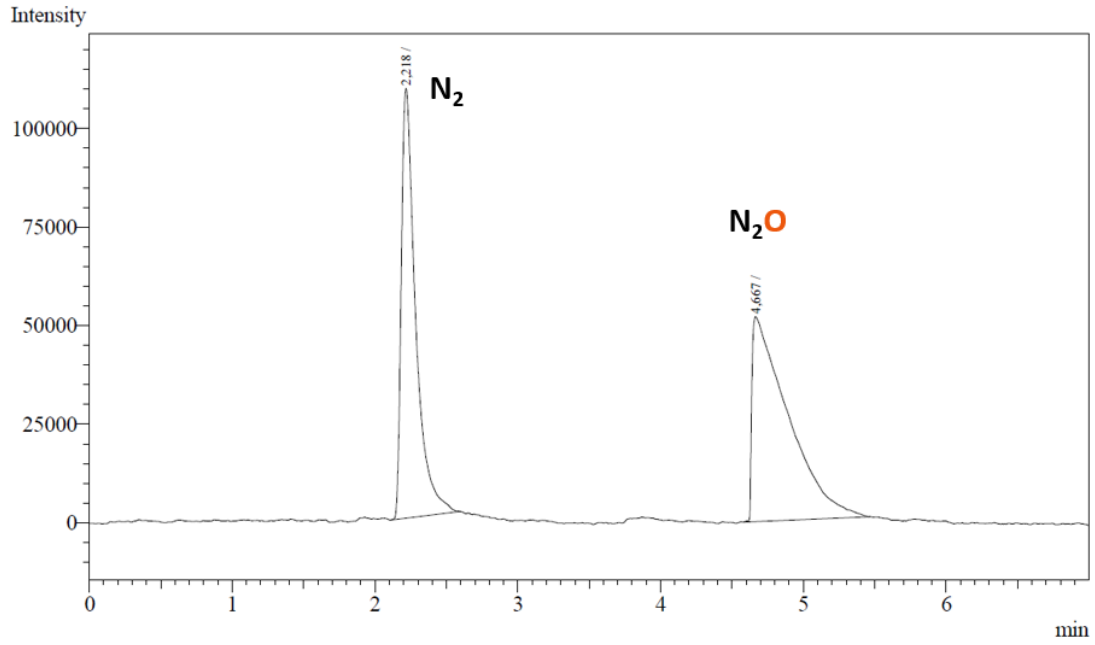

Figure S24: GC analysis of the gaseous phase after 5 h of irradiation, on a 1.2 mmol scale.

4.4.2 GC trace for the reduction of N_2O catalyzed by **Re-1** in presence of TEOA

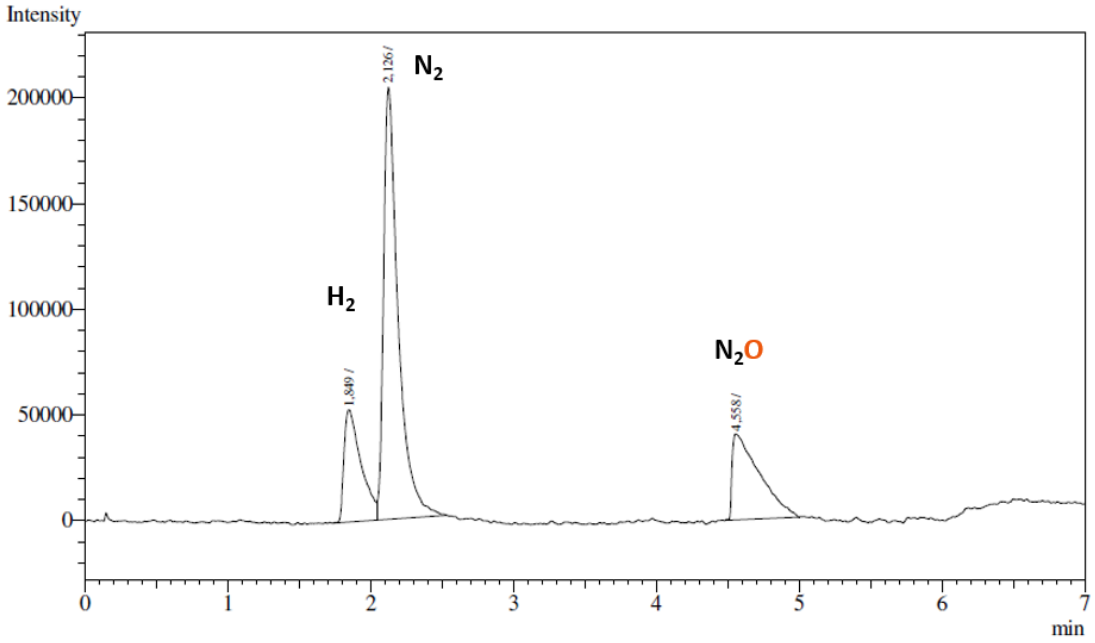

Figure S25: GC analysis of the gaseous phase after 2 h of irradiation.

4.4.3 GC traces for the control experiments for the photoreduction of N_2O with **Re-1** (see Table 1)

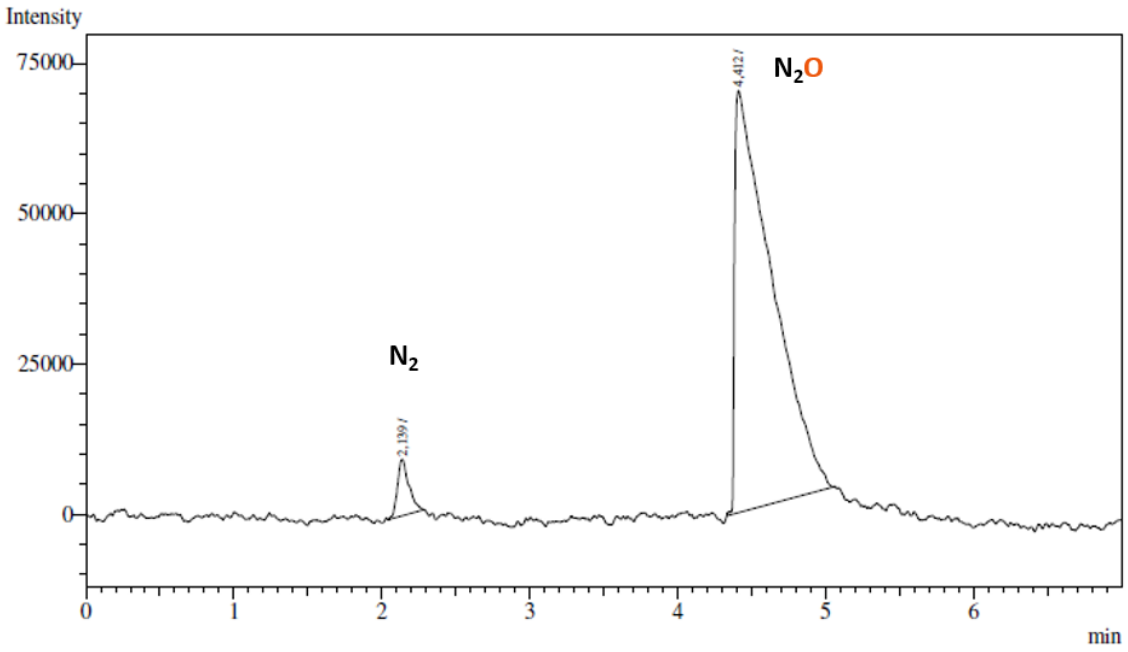

Figure S26: Control experiment without light.

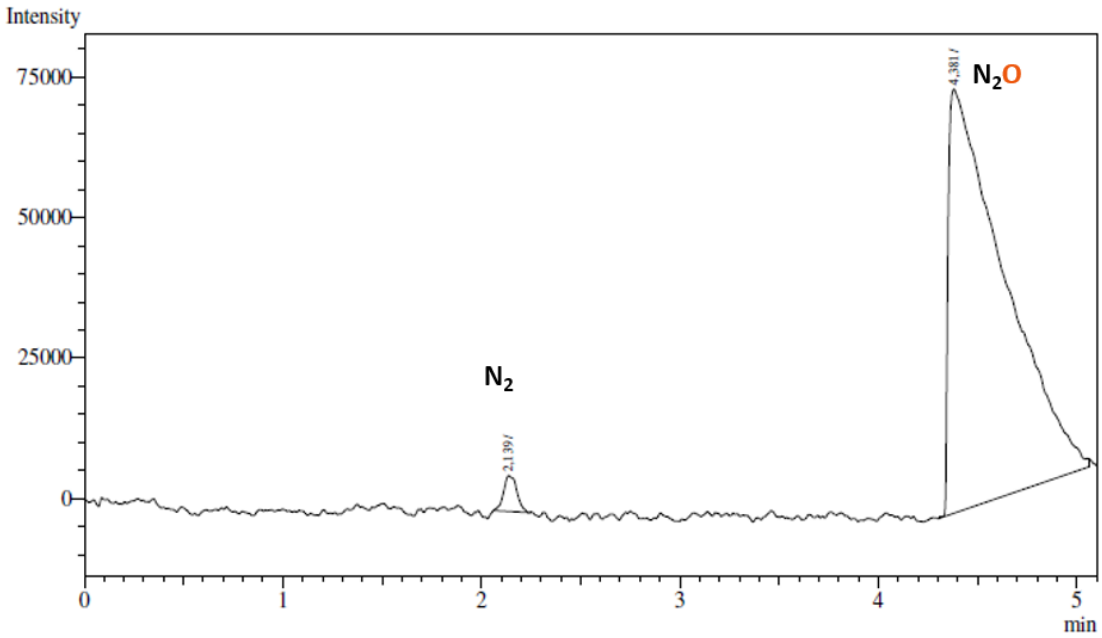

*Figure S27: Control experiment without **Re-1**.*

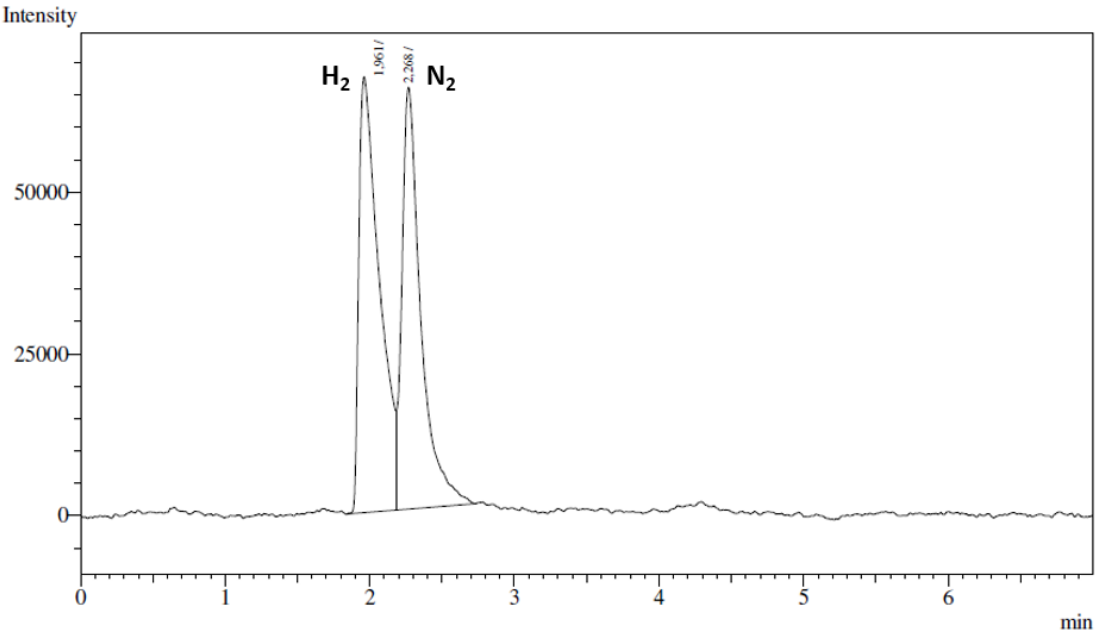

Figure S28: Control experiment with Ar instead of N_2O.

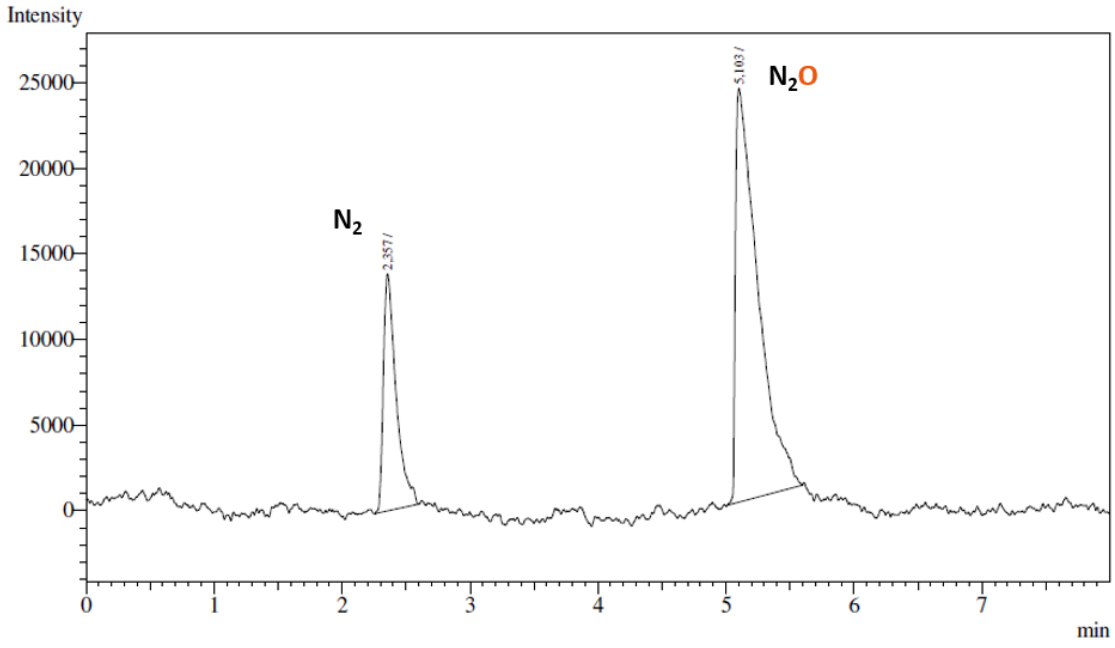

Figure S29: Control experiment without TEOA.

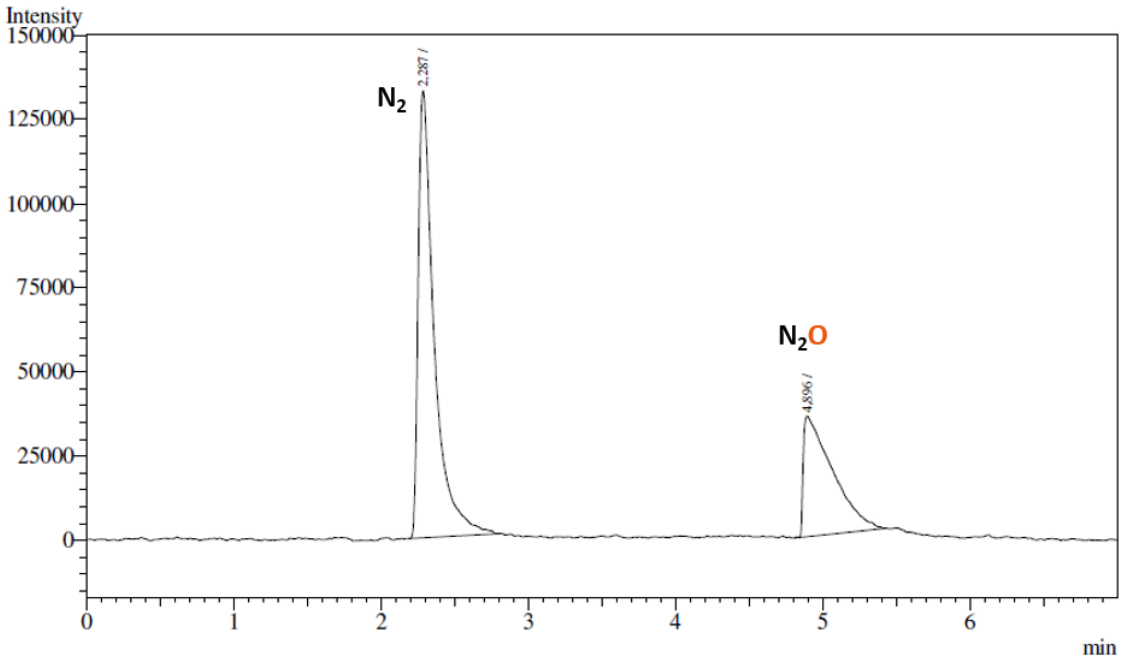

Figure S30: Control experiment with DIPEA instead of TEOA.

4.5 Copies of UV-Vis spectra

4.5.1 Absorption spectrum of **Re-4**

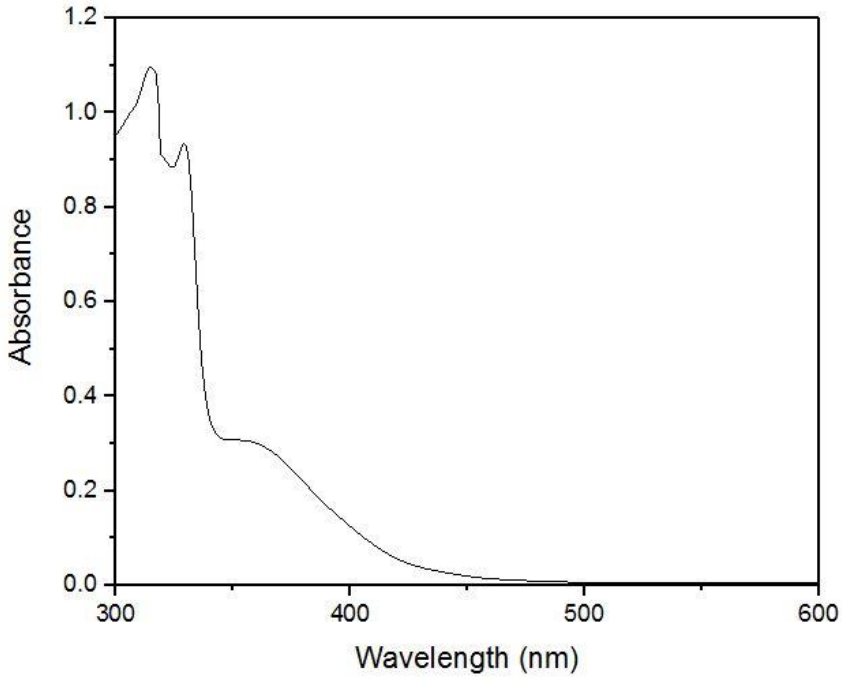

*Figure S31: Absorption spectrum of **Re-4** (175 µM in acetonitrile) at 293 K.*

4.5.2 Absorption spectrum of **Re-5**

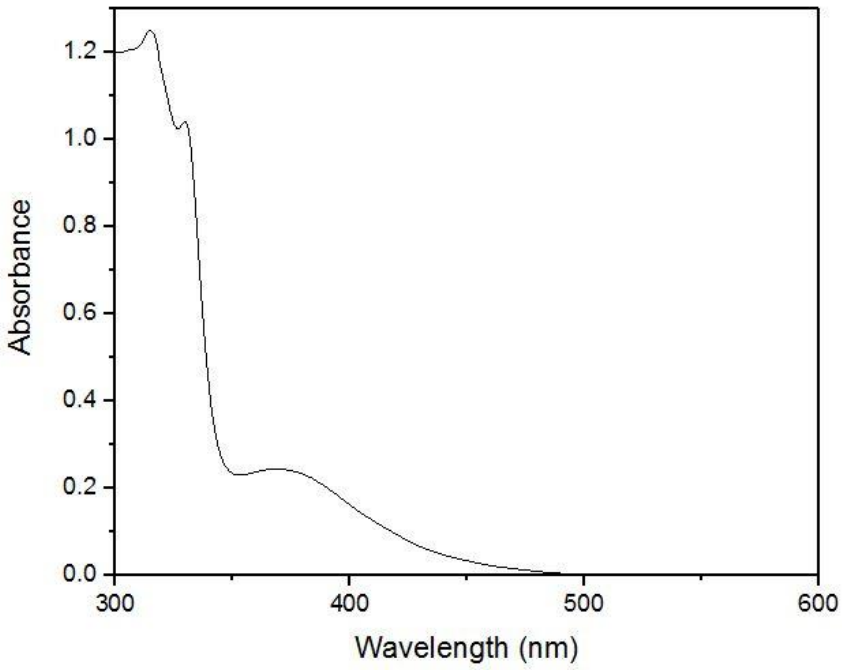

*Figure S32: Absorption spectrum of **Re-5** (175 µM in acetonitrile) at 293 K.*

5 References

1 H. Hori, J. Ishihara, K. Koike, K. Takeuchi, T. Ibusuki and O. Ishitani, *Chem. Lett.*, 1997, **26**, 1249-1250.

2 D. H. Gibson, X. Yin, H. He and M. S. Mashuta, *Organometallics*, 2003, **22**, 337-346.

3 J. M. Smieja and C. P. Kubiak, *Inorg. Chem.*, 2010, **49**, 9283-9289.

4 F. Adams, M. Pschenitza and B. Rieger, *ChemCatChem*, 2018, **10**, 4309-4316.

5 M. Schmittel, A. Ganz, W. A. Schenk and M. Hagel, *Zeitschrift für Naturforschung B*, 1999, **54**, 559-564.

6 Spectral Database for Organic Compounds (SDBS); http://sdbs.db.aist.go.jp/sbds/ (accessed July 29 2020). SDBS No. 518, 1824, 9994, 10015, 9996, and 5723

7 K. S. Kanyiva, Y. Nakao and T. Hiyama, *Angew. Chem. Int. Ed.*, 2007, **46**, 8872-8874.

8 *Apex3*, Madison, Wisconsin, USA, **2019**,

9 *Collect*, R. W. W. Hooft, The Netherlands, **1998**,

10 (a) *Saint*, Madison, Wisconsin, USA, **2019**, ; (b) [20] processing of x-ray diffraction data collected in oscillation mode, Z. Otwinowski and W. Minor, in *Methods enzymol.*, Academic Press, 1997, vol. 276, pp. 307-326.

11 (a) *Sadabs*, Madison, Wisconsin, USA, **2016**, ; (b) L. Krause, R. Herbst-Irmer, G. M. Sheldrick and D. Stalke, *J. Appl. Crystallogr.*, 2015, **48**, 3-10.

12 G. Sheldrick, *Acta Crystallographica Section A*, 2015, **71**, 3-8.

13 G. Sheldrick, *Acta Crystallographica Section C*, 2015, **71**, 3-8.

14 C. B. Hubschle, G. M. Sheldrick and B. Dittrich, *J. Appl. Crystallogr.*, 2011, **44**, 1281-1284.

15 L. Farrugia, *J. Appl. Crystallogr.*, 2012, **45**, 849-854.